Ab Initio and Density Functional Study of the Activation Barrier for Ethane Cracking in Cluster Models of Zeolite H-ZSM-5

S. A. Zygmunt,[†,‡] L. A. Curtiss,*[,‡] P. Zapol,[‡] and L. E. Iton[§]

Department of Physics and Astronomy, Valparaiso University, Valparaiso, Indiana 46383, and Argonne National Laboratory, Argonne, Illinois 60439

Received: September 9, 1999; In Final Form: December 7, 1999

Protolytic cracking of ethane in zeolites has been investigated using quantum-chemical techniques and a cluster model of the zeolite acid site. An aluminosilicate cluster model containing five tetrahedral (Si, Al) atoms (5T) was used to locate all of the stationary points along a reaction path for ethane cracking at the HF/6-31G(d), B3LYP/6-31G(d), and MP2(FC)/6-31G(d) levels of theory. The cracking reaction occurs via a protonated structure that is a carbonium-like ion and is a transition state on the potential energy surface. The activation barrier for cracking calculated at each level of theory was refined by including (i) vibrational energies at the experimental reaction temperature of 773 K, (ii) electron correlation and/or an extended basis set at the B3LYP/6-311+G(3df,2p) or MP2(FC)/6-311+G(3df,2p) levels, and (iii) the influence of the surrounding zeolite lattice from a 58T cluster model of the zeolite H-ZSM-5. The barrier is especially sensitive to the long-range electrostatic effect of the lattice, which reduces it by 14.5 kcal/mol from the value obtained with the 5T cluster. The final calculated barrier of 54.1 kcal/mol at the MP2(FC)/6-311+G(3df,2p)//MP2-(FC)/6-31G(d) level, including corrections, is significantly smaller than values obtained by previous theoretical studies and is in reasonable agreement with typical experimental values for short alkanes. The other levels of theory give similar values for the barrier.

I. Introduction

The transfer of a proton from the Brønsted acid site to an adsorbed hydrocarbon molecule is an important step in acid catalysis by zeolites. However, this process is not yet fully understood at an atomic level. In particular, the protonated species have not been well characterized, and it is not known whether proton transfer to an alkane leads to a carbonium-like ion that is a stable intermediate or a short-lived transition-state. It is difficult to obtain information on this question using spectroscopic techniques, but it can be addressed through the use of quantum chemical techniques.

Earlier notions of the mechanisms of hydrocarbon transformations in catalysis by zeolites were based on reasoning by analogy with traditional organic chemistry in liquid solution by strong acid catalysts.[1] These mechanisms assumed the involvement of discrete carbenium ions formed as intermediates via the protonation of alkenes. In the case of alkane activation, superacid chemistry in solution provided the model, with the carbenium ions being assumed to be derived from carbonium ions created by the protonation of C−C or C−H bonds. More recently, experimental evidence countering the notion that discrete carbenium ions exist as intermediates in zeolites has been advanced by Haw, Nicholas, and co-workers[2,3] using ^{13}C nuclear magnetic resonance (NMR) spectroscopy. These species were concluded to exist in the zeolite, in contrast to the case of liquid superacids, as alkoxy-like species covalently bound to a framework oxygen atom. The conclusion was supported by complementary quantum chemical studies. As such, the alkoxy-like species represents the thermodynamically stable intermediate species, and the acid strengths of the zeolites were placed below that of 100% H_2SO_4. The situation with carbonium ions is more ambiguous because correspondingly definitive experimental data are not available. The matter is further confused by conflicting experimental data for acidic zeolites from alkane cracking,[4] dehydrogenation,[5] and hydrogen exchange[6] reactions, which proceed via carbonium ion intermediates in liquid superacid catalysis. In particular, these transformation reactions in alkanes over zeolites at moderate temperatures seem to involve chain propagation by bimolecular hydride transfer steps. The important point of contention centers on whether carbonium-like ion species are formed as stable intermediates (that may or may not be stabilized by the interaction with the zeolite) or are formed solely as transition state species.

Quantum chemical calculations at different levels of theory have provided support for both answers, viz., that the carbonium-like ion species exist only as transition state species[7−11] or that they are thermodynamically stable species occupying local minima on the potential energy surface.[11,12] These calculations have used small cluster models for the zeolite acid site that do not include a complete set of four neighboring oxygen atoms around the substitutional aluminum site. The most ambitious study to date used local density functional theory with a basis set similar to 6-31G(d) to examine ethane cracking in a cluster with three tetrahedral atoms (3T).[9] However, the activation barrier found in this study (77 kcal/mol) is significantly higher than typical experimental values for propane and *n*-butane over H-ZSM-5 (47 ± 3 kcal/mol).[13] Other calculations of the monomolecular cracking barrier for ethane have also given results in the range of 70−80 kcal/mol.[8,10] No experimental value for the ethane cracking barrier is available in the literature, so a direct comparison is not possible. However, since the values measured for *n*-alkanes from propane through hexane are essentially equal,[13] it is expected that the value for ethane should

[†] Valparaiso University. E-mail: stan.zygmunt@valpo.edu.
[‡] Materials Science and Chemistry Divisions, Argonne National Laboratory. E-mail: curtiss@anl.gov.
[§] Materials Science Division, Argonne National Laboratory.

10.1021/jp993194h CCC: $19.00 © 2000 American Chemical Society
Published on Web 02/11/2000

be similar. Because of the large discrepancy between experimental and calculated values of activation energies for cracking, no convincing conclusion can be drawn as to the nature of the carbonium-like ion species on the basis of theory.

The theoretical overestimate of the barrier may be due to several factors. First, our work[14,15] on the interaction of a water dimer with the Brønsted acid site in zeolites showed that when proton transfer takes place, there are important interactions between the protonated molecule and three of the four oxygens surrounding the Al site. These interactions need to be included in the cluster model used for studying reactions at acid sites. However, all of the previous studies of ethane cracking at an acid site have included at most three tetrahedral atoms and thus have included only two oxygen atoms in the cluster model. Second, the influence of the zeolite lattice on the barrier has not been included in these previous studies. We have found that the long-range electrostatic effect of the extended lattice has a significant influence on the deprotonation energy of an acid site.[16] Finally, the previous studies have been done with relatively small basis sets. We have found use of extended basis sets to be important for studying zeolite−adsorbate systems.[17] These are three possible deficiencies in the calculations that could cause the overestimate of the barrier.

The purpose of the present study was to investigate the potential energy surface for the monomolecular ethane cracking reaction at a zeolitic acid site in order to address the deficiencies discussed above and to attempt to provide a definitive conclusion as to the character of the carbonium-like ion species formed during this reaction. In our investigation of the potential energy surface, we have used a cluster model for the zeolite that includes a complete coordination shell of oxygens around the aluminum site. In addition, we have examined the importance of long-range electrostatic interactions on the reaction energetics by using cluster models containing up to 193 atoms. Finally, we have studied the importance of larger basis sets and electron correlation on the activation barrier. In section II we discuss the theoretical methods and zeolitic cluster models used. In section III we present and discuss results for the ethane cracking reaction pathway. In section IV conclusions are drawn.

II. Theoretical Methods

We have used ab initio molecular orbital theory[18,19] and gradient-corrected density functional theory[20,21] in this investigation of the ethane cracking reaction. An $Si_4AlO_4H_{13}$ cluster was used for the potential energy search of this reaction. It is centered on the aluminum atom and has hydrogen termination of the silicons. It is referred to as a 5T cluster because it has five tetrahedral (Si, Al) atoms. The reaction pathway from ZOH + C_2H_6 to $ZOCH_3$ + CH_4 (ZO = 5T zeolitic cluster) was investigated at the HF/6-31G(d), B3LYP/6-31G(d), and MP2-(FC)/6-31G(d) levels of theory by locating all of the local minima and transition states along a pathway for proton transfer and cracking. Full optimizations were carried out for all stationary points. The vibrational frequencies of all of the stationary points were calculated and confirmed that the local minima had all positive frequencies. The transition states that were located had only one imaginary vibrational frequency corresponding to the reaction coordinate. We verified the connectivity of the structures on the potential energy surface by displacing the atoms in each transition state complex along the calculated reaction coordinate and then optimizing the resulting structures. In each case, this optimization led to the local energy minimum structures on either side of the transition state. This is similar to the method for verifying connectivity between stationary states on a potential surface used in a recent computational study of bimolecular cracking of alkanes.[22]

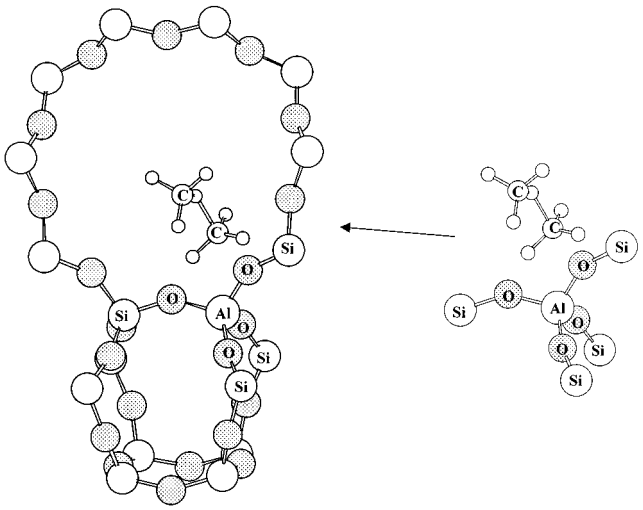

Figure 1. Illustration of the embedding procedure used to estimate long-range effects of the zeolite lattice. In this figure the 5T cluster model of the cracking transition state is shown embedded in the 18T cluster. A similar procedure is used for the larger clusters.

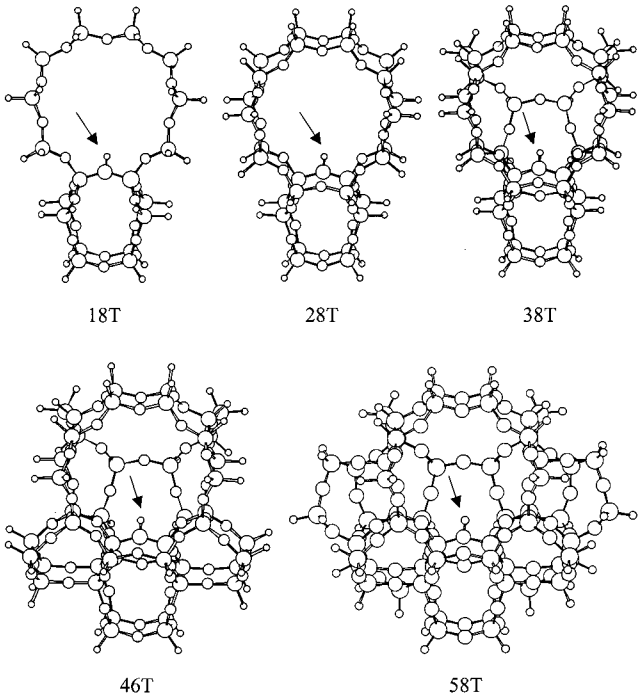

Figure 2. Structures of 18T, 28T, 38T, 46T, and 58T clusters used for calculation of long-range electrostatic effects on the barrier energy for ethane cracking. The arrow indicates the location of the acidic proton in each cluster.

To obtain a better estimate of the activation barrier for cracking, we have added several corrections to the results obtained at each level of theory. In addition to the standard correction for zero-point vibrational energies (ΔZPE), a vibrational energy correction at the experimental reaction temperature of 773 K (ΔE_{773}) was calculated. These corrections were calculated using the recommended scaling factors for frequencies at each level of theory.[23] Next, a correction for the effects of electron correlation and/or an extended basis set, Δ(higher level theory), was calculated at the B3LYP/6-311+G(3df,2p) or MP2-(FC)/6-311+G(3df,2p) level. Finally, we calculated an approximate correction for the small cluster size of our model by

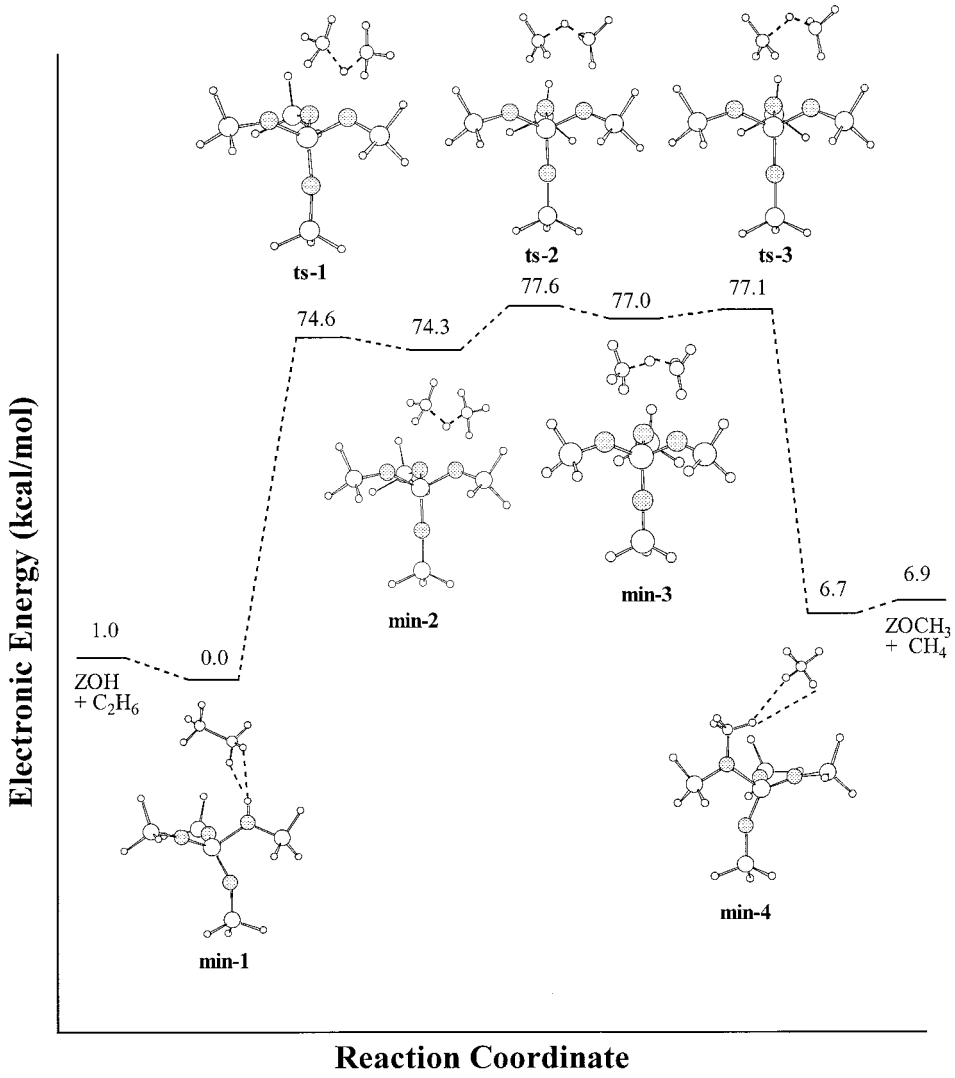

Figure 3. HF/6-31G(d) potential energy surface for protolytic cracking of ethane by a zeolitic acid site. Relative electronic energies are in kcal/mol.

using larger clusters with rigid experimental geometries. This correction, Δ(long-range), reflects the long-range electrostatic influence of the H-ZSM-5 lattice on the barrier energy.

The long-range electrostatic correction was determined by calculating the "true" activation energy (i.e., the energy difference between the adsorbed ethane molecule and the cracking transition state) at the HF/6-31G(d) level using much larger clusters. We used a procedure in which geometries from a 5T cluster are embedded in much larger zeolitic clusters with no further geometry optimization. An 18T cluster model of H-ZSM-5 with an embedded 5T cluster is depicted in Figure 1. The atomic positions in these larger clusters, which contain 18, 28, 38, 46, and 58 T atoms, were derived from experimental diffraction studies of orthorhombic H-ZSM-5.[24] These cluster models are shown in Figure 2. Apart from 58T, these are the same clusters that we used to investigate the cluster size dependence of calculated deprotonation energies in H-ZSM-5 at a lower level of theory.[16] An Al atom was substituted for Si at the T12 site to form a model for the Bronsted acid site. The six intermolecular geometrical parameters describing the positions of the C_2H_6 relative to the rigid cluster were obtained from an optimization of these parameters for a rigid C_2H_6 molecule in a rigid 5T cluster. In this optimization the internal C_2H_6 geometry was taken from the full optimization of the 5T $ZOH\cdots C_2H_6$ complex and the atomic positions of the 5T cluster were taken from the experimental geometry of H-ZSM-5. The six intermolecular parameters and the same C_2H_6 geometry were then used to calculate total energies of successively larger cluster models of the adsorbed complex, $ZOH\cdots C_2H_6$. A similar procedure was used for the $C_2H_7^+$ cracking transition state, $ZO^-\cdots C_2H_7^+$. These total energies were then used to determine the effect on the calculated barrier energy. The change in the activation barrier due to the increase in cluster size from 5T to the largest model, 58T, is an estimate of the long-range electrostatic influence of the zeolite lattice in a real crystal.

III. Results and Discussion

A. Potential Energy Surface for C_2H_6 Cracking Reaction. The equilibrium and transition state structures located at the three levels of theory used in this study are shown in Figures 3 and 4, along with schematic potential energy surfaces for protolytic cracking of ethane along this reaction path. The relative energies of the equilibrium and transition structures are listed in Table 1 for each method of geometry optimization, along with corrections to the relative energies obtained by including the effects of basis set extension and electron correlation.

The initial structure, **min-1** ($ZOH\cdots C_2H_6$), corresponds to ethane adsorbed at an acid site on the 5T structure. Three transition states on the potential energy surface for cracking of ethane have been located at the HF/6-31G(d) level. The first transition state, **ts-1**, is for proton transfer from the zeolite to

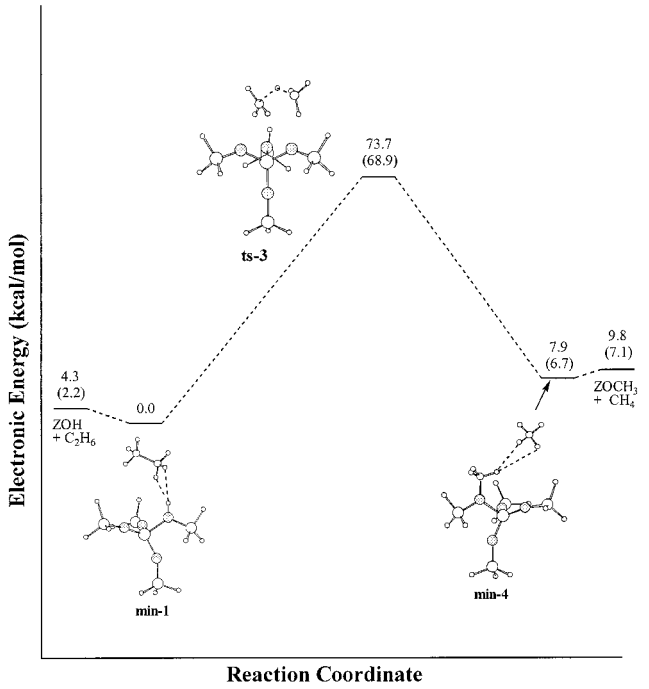

Figure 4. Potential energy surface for protolytic cracking of ethane by a zeolitic acid site from correlated calculations. Relative electronic energies are shown at the MP2(FC)/6-31G(d) and B3LYP/6-31G(d) (in parentheses) levels of theory in kcal/mol.

ethane ($ZO^-\cdots H^+\cdots C_2H_6$) to form an ion-pair complex ($ZO^-\cdots C_2H_7^+$, **min-2**). In our notation ZO^- represents the zeolite framework fragment with the acidic proton removed. In the **min-2** complex the CC distance increases slightly from its value in **ts-1**. A further increase of the CC distance and rotation of the adsorbed species about the CC axis produces a second transition state, **ts-2**, in which the acidic proton is now considerably further away from the zeolite framework. The **ts-2** complex is connected to another equilibrium structure, **min-3**, in which the proton is slightly closer to one C atom than the other. The third transition state, **ts-3** ($ZO^-\cdots H_3CH^+CH_3$), leads directly to formation of CH_4 weakly adsorbed on the zeolite and a covalently bound methoxy-like species ($ZOCH_3\cdots CH_4$, **min-4**). In $ZOCH_3$ the acidic proton of ZOH has been replaced by a methyl cation.

The HF/6-31G(d) activation barrier for proton transfer (**min-1** → **ts-1**), neglecting zero-point energy corrections, is 74.6 kcal/mol (see Table 1). The $Z^-\cdots H_3CH^+CH_3$ transition state (**ts-3**), which leads to cracking, is located 77.1 kcal/mol above **min-1**. The ion-pair complex (**min-2**) formed by proton transfer is only 0.3 kcal/mol lower in energy than the transition state (**ts-1**). However, when zero-point energies are included, the **min-2** structure is actually 0.6 kcal/mol *higher* in energy than the **ts-1** structure. Likewise, the **min-3** structure is 0.3 kcal/mol higher than the **ts-3** structure. This suggests that **min-2** and **min-3** are not true stable equilibrium structures. Table 1 also shows that when single point B3LYP/6-311+G(3df,2p) corrections to the HF/6-31G(d)//HF/6-31G(d) energies are included, **min-2** is actually 2.9 kcal/mol *higher* in energy than **ts-1** (3.7 kcal/mol with zero-point energies). A similar effect can be seen by comparing the relative energies of the **ts-2** and **min-3** structures. These results suggest that the **min-2** and **min-3** local minima should disappear at higher levels of theory. Although the **ts-3** structure is 0.5 kcal/mol lower in energy than the **ts-2** structure at the HF/6-31G(d) level, it is actually 0.9 kcal/mol *higher* in energy (0.8 kcal/mol with zero-point energies) when the basis set and correlation corrections are included. When B3LYP/6-311+G(3df,2p) corrections to the HF/6-31G(d)//HF/6-31G(d) energies are included, the results in Table 1 indicate that the "true" energy barrier for ethane cracking corresponds to the energy difference between the **min-1** and **ts-3** structures. This activation barrier is 69.1 kcal/mol (66.8 kcal/mol including zero-point energies).

At the B3LYP/6-31G(d) and MP2(FC)/6-31G(d) levels, which include electron correlation effects, we did not find stationary points corresponding to the HF/6-31G(d) **ts-1**, **min-2**, **ts-2**, or **min-3** structures shown in Figure 3. The only structures that are stationary points on the potential surface at correlated levels of theory are **min-1**, **ts-3**,[26] and **min-4** as shown in Figure 4. This is consistent with the results based on HF/6-31G(d) geometries in Table 1, which indicate that the **min-2** and **min-3** stationary points disappear when higher levels of theory are included. The **min-1** and **ts-3** structures are shown in Figure 5, with selected optimized geometrical parameters at different levels of theory. It can be seen from the **min-1** structure that the correlated levels of theory (B3LYP and MP2) produce shorter distances (~2.0 Å) between the acidic proton and the adsorbed ethane molecule than the HF level of theory (~2.3 Å). However, MP2 yields a much shorter distance between the framework oxygen atom adjacent to the acid site and the nonbonding end of the ethane molecule (~2.8 Å) than B3LYP or HF (~4.0 Å). This reflects the inability of B3LYP to adequately account for weak van der Waals interactions such as hydrocarbon adsorption in zeolites.[25] The geometries of the **ts-3** structure are similar at all three levels of theory. The $C_2H_7^+$ fragment has a somewhat different structure from the nonclassical free carbonium ion, in which the proton is equidistant from the two carbon atoms. In the **ts-3** structure the $C-H^+$ distances are 1.37 and 1.17 Å at the MP2(FC)/6-31G(d) level compared to 1.22 Å in the free ion at the MP2(FU)/6-31G(d,p) level of theory.[27] At the B3LYP/6-31G(d) and MP2(FC)/6-31G(d) levels the barrier is 68.9 and 73.7 kcal/mol, respectively (66.5 and 71.7 kcal/mol with zero-point energies). Including the effects of the 6-311+G(3df,2p) basis set reduces these values to 68.6 and 71.7 kcal/mol (66.2 and 69.7 with zero-point energies). Thus, the three levels of theory give activation barriers in the range 66−70 kcal/mol (including zero-point energies). However, these calculated values are much larger than the experimental value[13] of 47 ± 3 kcal/mol for propane and *n*-butane in H-ZSM-5 at 773 K. As discussed earlier, the ethane barrier is expected to be similar. In the following section we describe a possible reason for the remaining discrepancy between experiment and theory.

B. Influence of Long-Range Electrostatic Interactions on the Cracking Barrier. The long-range electrostatic effect of the H-ZSM-5 lattice on the calculated cracking barrier was investigated using the embedding method (Figure 1) described in section II. The calculations were based on the HF/6-31G(d) optimized 5T geometries for **min-1** and **ts-3** and the larger cluster models (18T, 28T, 38T, 46T, and 58T) of the zeolite framework shown in Figure 2. The change in the cracking energy barrier (relative to the 5T cluster) resulting from this embedding procedure is shown in Table 2. The value for the 58T cluster is currently our best approximation for the electrostatic influence of the zeolite lattice on the barrier energy. We are continuing to explore this effect with even larger cluster models.

A summary of the calculated cracking barriers, including the long-range electrostatic effect from the 58T cluster, is given in Table 3. The other corrections from section III.A (correlation, basis set extension, and zero-point energies), as well as the vibra-

TABLE 1: Relative Energies for Stationary Points on Ethane Cracking Reaction Pathway

	relative energy,[b] kcal/mol					
structure[a]	HF/6-31G(d) //HF/6-31G(d)	B3LYP/ 6-311+G(3df,2p)// HF/6-31G(d)	B3LYP/6-31G(d)// B3LYP/6-31G(d)	B3LYP/ 6-311+G(3df,2p)// B3LYP/6-31G(d)	MP2(FC)/6-31G(d)// MP2(FC)/6-31G(d)	MP2(FC)/ 6-311+G(3df,2p)// MP2(FC)/6-31G(d)
$ZOH + C_2H_6$	1.0 (0.5)	1.3 (0.8)	2.2 (1.4)	1.6 (0.8)	4.3 (3.4)	5.2 (4.3)
min-1	0.0 (0.0)	0.0 (0.0)	0.0 (0.0)	0.0 (0.0)	0.0 (0.0)	0.0 (0.0)
ts-1	74.6 (72.6)	60.0 (58.0)				
min-2	74.3 (73.2)	62.9 (61.7)				
ts-2	77.6 (75.4)	68.2 (66.0)				
min-3	77.0 (75.1)	68.3 (66.5)				
ts-3	77.1 (74.8)	69.1 (66.8)	68.9 (66.5)	68.6 (66.2)	73.7 (71.7)	71.7 (69.7)
min-4	6.7 (5.9)	9.9 (9.1)	6.7 (5.7)	10.1 (9.1)	7.9 (7.0)	10.6 (9.8)
$ZOCH_3 + CH_4$	6.9 (5.9)	9.8 (8.8)	7.1 (5.7)	9.7 (8.4)	9.8 (8.2)	12.8 (11.3)

[a] Structures are shown in Figures 3 and 4. [b] Values in parentheses include zero-point energies. Scaling factors are 0.9135 (HF), 0.9806 (B3LYP), and 0.9670 (MP2).

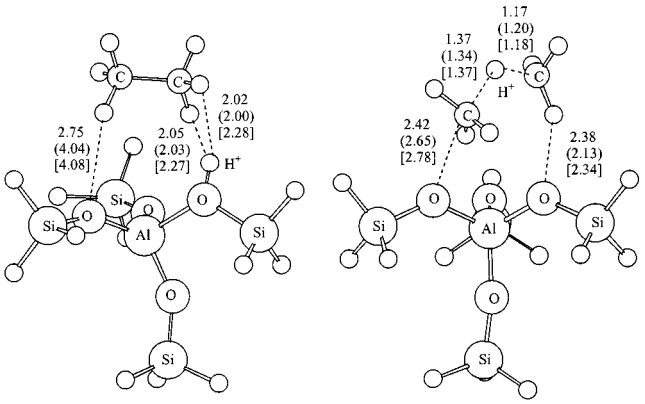

Figure 5. Structures of the adsorbed ethane complex (**min-1**) and the cracking transition state (**ts-3**) with selected geometrical parameters obtained from optimizations at the MP2(FC)/6-31G(d), B3LYP/6-31G(d) (in parentheses), and HF/6-31G(d) [in brackets] levels of theory.

TABLE 2: Long-Range Electrostatic Correction for the Ethane Cracking Barrier (min-1 → ts-3) for Various Cluster Models of H-ZSM-5 Relative to the 5T Cluster[a]

cluster size[b]	O:T ratio[c]	change in barrier, kcal/mol
18T ($Si_{17}AlO_{22}H_{29}$)	1.22	−7.6
28T ($Si_{27}AlO_{40}H_{33}$)	1.43	−7.9
38T ($Si_{37}AlO_{54}H_{45}$)	1.42	−12.7
46T ($Si_{45}AlO_{68}H_{49}$)	1.48	−14.0
58T ($Si_{57}AlO_{88}H_{57}$)	1.52	−14.5

[a] HF/6-31G(d) calculations (see text and Figure 2 for description of geometries). [b] The stoichiometry listed is for the ZOH cluster. [c] T denotes number of tetrahedral atoms (Si and Al).

tional correction to 773 K, are also included in this table. Note that the higher level theory correction is much larger for the HF case than for B3LYP and MP2 because it includes both electron correlation and basis set extension, while the latter two corrections include only the basis set extension. Assuming additivity of these various corrections, the energy barrier for ethane cracking is calculated to be in the range 51−54 kcal/mol. The MP2 result of 54.1 kcal/mol is probably most accurate, since the MP2 method is more accurate than the B3LYP method for calculating the adsorption energy of hydrocarbon molecules in zeolites. The energies in Table 1 show that when higher level theory and zero-point energies are included, the MP2 adsorption energy for ethane at the acid site (4.3 kcal/mol) is significantly greater than the B3LYP value (0.8 kcal/mol). The poor performance of density functional theory for hydrocarbon adsorption energies in zeolites has been noted previously.[25] Our result for the barrier compares quite reasonably to the experimental value of 47 ± 3 kcal/mol for propane and *n*-butane in H-ZSM-5.[13]

TABLE 3: Barrier Energy for min-1 → ts-3 from Calculations on 5T Cluster and Energy Corrections

	energies, kcal/mol		
geometry	HF/6-31G(d)	B3LYP/ 6-31G(d)	MP2(FC)/ 6-31G(d)
ΔE(**min-1** → **ts-3**)[a]	77.1	68.9	73.7
Δ(higher level theory)	−8.0[b]	−0.3[c]	−2.0[d]
ΔZPE[e]	−2.1	−2.4	−2.0
ΔE_{773}[f]	−1.2	−1.1	−1.1
Δ(long-range)[g]	−14.5	−14.5	−14.5
total	51.3	50.6	54.1

[a] Energy of **ts-3** structure relative to **min-1** structure, i.e., barrier for ethane cracking. [b] B3LYP/6-311+G(3df,2p)//HF/6-31G(d) correction. [c] B3LYP/6-311+G(3df,2p)//B3LYP/6-31G(d) correction. [d] MP2(FC)/6-311+G(3df,2p)//MP2(FC)/6-31G(d) correction. [e] Correction for zero-point energy. Scaling factors are 0.9135 (HF), 0.9806 (B3LYP), and 0.9670 (MP2) from ref 23. [f] Correction for vibrational energy at 773 K. Scaling factors are 0.8829 (HF), 0.9816 (B3LYP), and 0.9743 (MP2) from ref 23. [g] HF/6-31G(d) correction for 58T cluster model of H-ZSM-5 (from Table 2).

TABLE 4: Mulliken Charges (in e) for Adsorbates in ts-3 and min-1 Structures

adsorbate	HF/6-31G(d)	B3LYP/6-31G(d)	MP2(FC)/6-31G(d)
C_2H_7 (**ts-3**)	0.90	0.81	0.88
C_2H_6 (**min-1**)	0.01	0.03	0.00

The long-range electrostatic effect of the zeolite lattice causes a surprisingly large reduction in the barrier due to the electrostatic stabilization of the ionic transition state, **ts-3**, relative to the initial adsorbed complex, **min-1**, which has very little charge transfer between the zeolite and the adsorbate. The net Mulliken charges for the adsorbates in the **ts-3** and **min-1** 5T structures are listed in Table 4 at various levels of theory. The net Mulliken charge on the C_2H_7 fragment of the **ts-3** structure is approximately +0.9e, which suggests that it is an ion-pair complex. The **ts-3** transition state has a dipole moment of 11.09 D compared to 5.03 D for the **min-1** adsorbed structure. (These dipole moments are for the entire system of the zeolite cluster and adsorbate.) Thus, the polar zeolite framework has a "solvation" effect that stabilizes the species with the larger dipole moment relative to the one with a smaller dipole moment. If one assumes a dielectric constant of 2.5 for H-ZSM-5 and applies the SCI-PCM solvation model[28] to the 5T structures, the energy of the transition structure **ts-3** is stabilized by 4.3 kcal/mol relative to the equilibrium structure **min-1**. This result, though only approximate, is consistent with the results based on the use of the 58T cluster for the H-ZSM-5 structure.

There are a number of approximations used in this study of the barrier for ethane cracking that may affect our results. One

is the lack of complete geometry optimization in the clusters used to assess the long-range electrostatic effects. In addition, these clusters have O:T ratios of about 1.5 compared to an O:T atom ratio of 2 for bulk H-ZSM-5 (see Table 2). As mentioned above, we have also assumed the additivity of the corrections shown in Table 3. We estimate that these approximations may introduce as much as 5 kcal/mol error into our final calculated barrier.

C. Comparison with Previous Theoretical Calculations. As mentioned in the Introduction, there have been a number of studies of *n*-alkane cracking in zeolites. Van Santen et al.[9] studied ethane cracking with a 3T cluster using local density functional theory and a basis set similar to 6-31G(d). They found two possible pathways for ethane cracking. One of their cracking transition states had a structure very similar to the one that we have found. However, the true activation barrier found in this study (77 kcal/mol) is significantly larger than the 69 kcal/mol that we found for the 5T cluster with the B3LYP/6-31G(d) density functional method. The difference may be due to their use of a *local* density method and/or their use of a smaller cluster.

Collins and O'Malley[11] studied *n*-butane cracking using the BLYP/3-21G* method with a 1T cluster model and found an ion-pair structure to be a local minimum on the potential energy surface. However, with a 3T cluster model they found such a structure to be a transition state instead. Their calculated activation energy for cracking was roughly 50% higher than the experimental value. Kazansky et al.[12] studied the interaction of ethane and *n*-butane with a 1T zeolite cluster model and in each case found an ion-pair structure to be a local minimum using the MP2/6-31G(d) method. In a different study, Kazansky et al.[8] used a 3T cluster at the HF/6-31G(d) level and found a transition state for ethane cracking with an activation energy of 83 kcal/mol. Our HF/6-31G(d) barrier of 77 kcal/mol for the 5T cluster (Table 1) is significantly lower than that found by Kazansky et al. The difference is probably due to our use of a full coordination shell of oxygens around the aluminum atom. Kazansky's corrections for zero-point energies and the MP2/6-31++G(d,p) level of theory resulted in a barrier of 75.4 kcal/mol. The reduction is similar in magnitude to what we found with inclusion of correlation and use of a larger basis set. Our work additionally includes the long-range effect of the zeolite lattice on the activation barrier, which was not considered in any of the earlier studies.

IV. Conclusions

We have investigated the protolytic cracking of ethane in cluster models of the zeolite H-ZSM-5. An aluminosilicate cluster containing five tetrahedral (Si, Al) atoms was used to locate stationary points along a reaction path for ethane cracking. Full geometry optimizations at the HF/6-31G(d), B3LYP/6-31G(d), and MP2(FC)/6-31G(d) levels of theory reveal that the reaction occurs via a protonated structure that is a transition state on the potential energy surface and leads to formation of methane and a covalently bound methoxy-like species. The calculated barriers were refined by including corrections for higher level theory, vibrational energies, and long-range electrostatic interaction. The final calculated barrier of 54.1 kcal/mol at the MP2(FC)/6-311+G(3df,2p)//MP2(FC)/6-31G(d) level, including corrections, is in reasonable agreement with experimental values for similar systems such as propane and *n*-butane. Previous calculations of ethane cracking barriers have been in the range 70−80 kcal/mol, which are much higher than expected from experiment. This study has shown that the barrier is especially sensitive to long-range electrostatic effects, which reduce it by as much as 14.5 kcal/mol from the value obtained with a 5T cluster.

Acknowledgment. This work was supported by the Division of Materials Sciences, Office of Basic Energy Sciences, Department of Energy, under Contract No. W-31-109-ENG-38. The authors gratefully acknowledge use of advanced computational facilities at the National Energy Research Scientific Computing Center and the Argonne Center for Computer Science and Technology. S.A.Z. acknowledges support from Valparaiso University for a research leave in 1997−98.

References and Notes

(1) Poutsma, M. L. In *Zeolite Chemistry and Catalysis*; Rabo, J. A., Ed.; ACS Monograph No. 171; American Chemical Society: Washington, DC, 1976; Chapter 8.

(2) Haw, J. F.; Richardson, B. R.; Oshiro, I. S.; Lazo, N. D.; Speed, A. J. *J. Am. Chem. Soc.* **1989**, *111*, 2052.

(3) Haw, J. F.; Nicholas, J. B.; Xu, T.; Beck, L. W.; Ferguson, D. B. *Acc. Chem. Res.* **1996**, *29*, 259.

(4) Kwak, B. S.; Sachtler, W. M. H.; Haag, W. O. *J. Catal.* **1994**, *149*, 465.

(5) Krannila, H.; Haag, W. O.; Gates, B. C. *J. Catal.* **1992**, *135*, 115.

(6) Sommer, J.; Hachoumy, M.; Garin, F.; Barthomeuf, D. *J. Am. Chem. Soc.* **1994**, *116*, 5491.

(7) Kazansky, V. B.; Senchenya, I. N.; Frash, M.; van Santen, R. A. *Catal. Lett.* **1994**, *27*, 345.

(8) Kazansky, V. B.; Frash, M. V.; van Santen, R. A. *Appl. Catal.* **1996**, *A146*, 225.

(9) Blaszkowski, S. R.; Nascimento, M. A. C.; van Santen, R. A. *J. Phys. Chem.* **1996**, *100*, 3463.

(10) Rigby, A. M.; Kramer, G. J.; van Santen, R. A. *J. Catal.* **1997**, *170*, 1.

(11) Collins, S. J.; O'Malley, P. J. *Chem. Phys. Lett.* **1995**, *246*, 555.

(12) Kazansky, V. B.; Frash, M. V.; van Santen, R. A. *Catal. Lett.* **1997**, *48*, 61.

(13) Narbeshuber, T. F.; Vinek, H.; Lercher, J. A. *J. Catal.* **1995**, *157*, 388.

(14) Olson, D. H.; Zygmunt, S. A.; Erhardt, M. K.; Curtiss, L. A.; Iton, L. E. *Zeolites* **1997**, *18*, 347.

(15) Zygmunt, S. A.; Curtiss, L. A.; Iton, L. E. To be submitted.

(16) Brand, H. V.; Curtiss, L. A.; Iton, L. E. *J. Phys. Chem.* **1993**, *7*, 12773.

(17) Zygmunt, S. A.; Curtiss, L. A.; Iton, L. E.; Erhardt, M. K. *J. Phys. Chem.* **1996**, *100*, 6663. Zygmunt, S. A.; Mueller, R. M.; Curtiss, L. A.; Iton, L. E. *THEOCHEM* **1998**, *9*, 430.

(18) Hehre, W. J.; Radom, L.; Pople, J. A.; Schleyer, P. V. R. *Ab Initio Molecular Orbital Theory*; John Wiley: New York, 1987.

(19) Frisch, M. J.; Trucks, G. W.; Schlegel, H. B.; Gill, P. M. W.; Johnson, B. G.; Robb, M. A.; Cheeseman, J. R.; Keith, T. A.; Petersson, G. A.; Montgomery, J. A.; Raghavachari, K.; Al-Laham, M. A.; Zakrzewskiv, V. G.; Ortiz, J. V.; Foresman, J. B.; Cioslowski, J.; Stefanov, B. B.; Nanayakkara, A.; Challacombe, M.; Peng, C. Y.; Ayala, P. Y.; Chen, W.; Wong, M. W.; Andres, J. L.; Replogle, E. S.; Gomperts, R.; Martin, R. L.; Fox, D. J.; Binkley, J. S.; Defrees, D. J.; Baker, J.; Stewart, J. P.; Head-Gordon, M.; Gonzales, C.; Pople, J. A. *Gaussian 94*; Gaussian, Inc.: Pittsburgh, PA, 1995.

(20) Becke, A. D. *J. Chem. Phys.* **1993**, *98*, 5648.

(21) Stephens, P. J.; Devlin, F. J.; Chabalowski, C. F.; Frisch, M. J. *J. Phys. Chem.* **1994**, *98*, 11623.

(22) Frash, M. V.; Kazansky, V. B.; Rigby, A. M.; van Santen, R. *J. Phys. Chem. B* **1998**, *102*, 2232.

(23) Scott, A. P.; Radom, L. *J. Phys. Chem.* **1996**, *100*, 16502.

(24) van Konigsveld, H.; van Bekkum, H.; Jansen, J. C. *Acta Crystallogr.* **1987**, *B43*, 127.

(25) Curtiss, L. A.; Zygmunt, S. A.; Iton, L. E. In *Proceedings of the 12th International Zeolite Conference*; Treacy, M. M. J., Marcus, B. K., Bisher, M. E., Higgins, J. B., Eds.; Materials Research Society: Pittsburgh, PA, 1999; p 415.

(26) Even after over one hundred optimization cycles, the B3LYP/6-31G(d) **ts-3** structure did not satisfy all of the default convergence criteria in the Gaussian 94 program, although its energy was changing by less than 10^{-5} Ha. The frequency calculation based on this geometry resulted in only one imaginary frequency, which corresponded to the reaction coordinate.

(27) de M. Carneiro, J. W.; Schleyer, P. v. R.; Saunders, M.; Remington, R.; Schaefer, H. F.; Rauk, A.; Sorensen, T. S. *J. Am. Chem. Soc.* **1994**, *116*, 3483.

(28) Foresman, J. B.; Keith, T. A.; Wiberg, K. B.; Snoonian, J.; Frisch, M. J. *J. Phys. Chem.* **1996**, *100*, 16098.